Synchronous equilibrium model for the diffusion of mutually exclusive particles in a heterogeneous lattice of adsorption sites

Federico G. Pazzona,* Pierfranco Demontis, and Giuseppe B. Suffritti

Dipartimento di Chimica e Farmacia, Università degli Studi di Sassari and Consorzio Interuniversitario Nazionale per la Scienza e Tecnologia dei Materiali (INSTM), Unità di Ricerca di Sassari, via Vienna, 2, I-07100 Sassari, Italy

(Received 16 April 2013; published 21 June 2013)

Through straight synchronization and proper manipulation of a sequential Monte Carlo glass-forming rule introduced by Fröbose and Jäckle [J. Stat. Phys. **42**, 551 (1986)], we constructed a synchronous, non-glass-forming rule for diffusion of mutually exclusive particles in a lattice of adsorption sites. The rule satisfies detailed balance in the presence of both homogeneous and heterogeneous adsorption energies. Our model differs from the usual lattice-gas cellular automata diffusion rules in that the mutual exclusion holds on the lattice sites rather than on the channels which connect neighboring sites, and from the mass-conserving cellular automata rules in the use of a no-partitioning scheme. The first aim of this work is to show that, although some prescriptions in the synchronous rule are introduced just to allow that both detailed balance and mutual exclusion can coexist with synchronicity, the diffusion process produced by the rule is not anomalous so that the rule can be regarded as a diffusion model. We then compare the diffusion isotherms of several test systems with the ones obtained by means of sequential Monte Carlo simulations of Arrhenius jumps of particles on a lattice. Finally, we apply the rule to the case of a (100) fcc model surface and estimate the amount of time correlation in the migration process, and show that the synchronous rule produces higher correlations and slightly lower diffusivity than the sequential Monte Carlo counterpart.

DOI: 10.1103/PhysRevE.87.063306 PACS number(s): 47.11.Qr, 05.50.+q, 68.35.Fx, 87.55.K−

I. INTRODUCTION

Since the late 1940s cellular automata (CA) have been developed in various directions, ranging from the construction of machines able to imitate the human brain's behavior to the solution of partial differential equations and the modeling of chemical and physical phenomena by means of fictitious, discrete microscopic evolution rules which, averaged in space and time, provide a realistic picture of the emulated phenomena at the meso- and the macroscale [1]. In particular, lattice-gas cellular automata (LGCA) models of particles propagating and colliding in a discrete grid of sites are devoted to the solution of problems in hydrodynamics [2–6] (where collisions do preserve momentum) and diffusion theory [1,7,8] (where collisions do not need to preserve momentum). In the models referenced above, the particles use *channels* to travel from site to site in the lattice: if from each site there are ν possible directions of motion then there will be exactly ν channels at each site. The moving particles are subjected to an exclusion criterion such that every channel can host at most one particle, not more, so that each site holds at most ν particles.

If there is need to impose mutual exclusion on *sites* rather than on channels, then fully synchronous CA rules are probably not the best choice, due to the conflicts that arise when the particles' positions are updated in parallel. Giving up some synchronicity, the use of Margolus neighborhoods and partitioning techniques can be of remarkable help in solving such conflicts and allows the implementation of conservation laws [9,10] and general restraints (e.g., the form of the stationary distribution of states [11]), producing a so-called block cellular automaton.

Although partitioning strategies make the production of a cellular automaton with conserved quantities easier, it is legitimate to ask whether or not it is possible to produce a fully synchronous LGCA of mutually exclusive particles whose evolution rule satisfies detailed balance. Whereas in a sequential Monte Carlo update the implementation of the detailed balance criterion in the state-to-state transitions is straightforward [12–16], doing the same when the rule is parallel can turn out to be quite a hard task—on the one hand, the node states in a lattice require a certain degree of mutual independence in order to be updated synchronously; on the other hand, mutual exclusion (and all kinds of mutual interaction of course) introduces dependencies in the evolution rule to avoid superposition of particles on the same node.

In this work we present a synchronous model, satisfying detailed balance, of particles traveling on a lattice of sites where each site can bear one particle at most. Our work does not claim the present rule as the best method for simulating diffusion on a lattice. It is however, to our knowledge, the first successful attempt in the construction of a fully synchronous CA rule for particle diffusion where mass conservation, detailed balance, and mutual exclusion *on sites* coexist without conflicting with each other. This task is achieved by means of a nontrivial acceptance and rejection criterion applied on the trial displacements, selected synchronously at each time step by all the particles in the system, which involves the first neighbors of each site plus some second neighbors.

The paper is organized as follows. In Sec. II we describe how the rule is structured and how we derived it by manipulating the original sequential rule proposed by Fröbose and Jäckle [17]. In Sec. III we derive the mathematical form of the equilibrium distribution of configuration. In Secs. IV A and IV B we show that the macroscopic diffusion equations derived formally through standard techniques are Fickian, and that the numerical simulation of the rule over several test

*fpazzona@uniss.it

systems leads to Gaussian propagators, linear mean-square displacements in the long-time limit (except for the case of single-file diffusion, where as expected they increase proportionally to $\sqrt{t}$), no glassy behavior, and generally smaller diffusivities than the Arrhenius-jump Monte Carlo counterpart. Finally, in Sec. IV C we apply the synchronous rule to the case of surface diffusion on a (100) fcc lattice, and discuss the importance of time correlations in the migration process through comparison between the numerical values and a mean-field formulation (whose details are provided in the Appendix) of the self-diffusion coefficient.

II. DESCRIPTION OF THE RULE

The starting point for the construction of the proper evolution algorithm was a (serial) Monte Carlo (MC) *extended exclusion principle* rule introduced by Fröbose and Jäckle, [17] prescribing that a particle jump from a lattice site, say r, to any neighboring site, say r', is accepted if and only if (i) the destination site r' is empty, and (ii) the neighbors of site r' (except r of course) are empty as well. Noticeably, this rule can be applied synchronously to all the particles in the lattice with no occurrence of multiple occupancies. As a drawback, however, when switching from sequential to synchronous evolution, the lattice configuration space changes and the detailed balance is lost, with the result that the system converges to a stationary distribution of configurations that cannot be expressed in a closed form. In particular, several conflicts prevent the model from satisfying detailed balance, by making some transformations, say $A \to B$ (where both A and B appear with nonzero probability in the stationary distribution), irreversible. In those cases, one or several intermediate steps are needed to get back from B to A, i.e., $B \to C_1 \to \cdots \to C_n \to A$. In a one-dimensional string of sites, for example, such a conflict can be schematized as follows:

$$\underset{1\ 2}{\square\square\blacksquare\blacksquare\square\square} \underset{\Omega'}{\overset{\Omega}{\rightleftarrows}} \underset{1\quad 2}{\square\square\blacksquare\square\blacksquare\square}, \qquad \begin{matrix}\Omega = P(P_0 + P),\\ \Omega' = 0,\end{matrix} \tag{1}$$

where occupied and empty sites are represented with black and empty squares, respectively, and numbers under each site are particle identities. Ω and Ω' are respectively the probability of the direct and of the reverse transformation, with $P = P_{\leftarrow} = P_{\rightarrow}$ as the probability of a particle to point toward the left or the right direction, and P_0 as the probability of a particle to point toward the same site it occupies. The configuration in the right-hand side (RHS) of (1) is produced when both particles in the LHS are attempting a displacement to the right, or when particle 2 (the probability associated with this event is P^2) is pointing to the right and particle 1 is attempting no displacement (the probability associated is $P_0 P$). The reverse transformation is not possible since particle 2 cannot jump into the empty site at its left due to the presence of particle 1 in the target neighborhood. In order to recover the starting configuration, it is required to pass through the intermediate configuration $\square\blacksquare\square\square\blacksquare\square$ (obtained by moving particle 1 to the left), since from such a configuration particle 1 and particle 2 can point to the right and to the left, respectively, thus producing exactly the starting configuration in the LHS of (1). Unfortunately, one can readily check that the probability resulting from the two-step reverse transformation does not equal Ω. In other words, a straight synchronization of the Fröbose and Jäckle rule produces a model where the particles are mutually exclusive but the forward and backward transformation probabilities are unbalanced, whereas we are looking for a rule satisfying detailed balance in such a way that at equilibrium, when the lattice is homogeneous (i.e., the sites all have the same binding energy) and the particles interact solely by mutual exclusion, every one of all possible combinations of the particles in the lattice sites is sampled with the same probability. Such a rule can be obtained if conflicts like the one we described above are solved by means of the following three prescriptions, summarized graphically in Fig. 1 (when a particle makes a trial displacement toward some site, we will say that it *points* or alternatively *points to* that site):

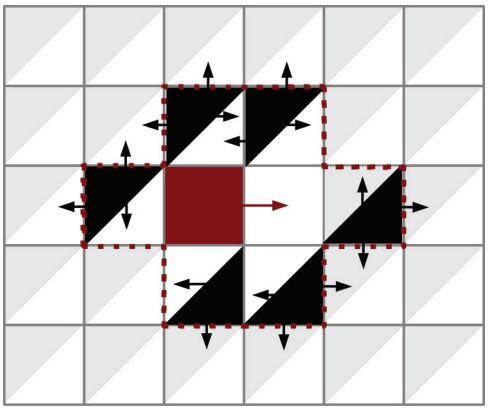

FIG. 1. (Color online) The evolution rule, sketched for a particle traveling in a square lattice where the neighborhood of each site is made by the first-neighboring sites only. In the present figure we display the case of the jump attempt of a particle (red square) into the site at its right (the pointing direction is represented by the red arrow). The cases of jump attempts in the up, the left, and the down directions can be obtained by simple rotation of the figure. The targeted site, called r', will be reached by the particle if it is empty, and if neither r' nor the particle is pointed to by any other particle. The latter condition is represented by the half-filled sites (around the red particle and the targeted site) equipped with arrows pointing toward any allowed direction but the one leading to the red particle or to the targeted site. Every half-filled square with arrows represents a site which can be empty or occupied by a particle pointing in any of the directions indicated by the arrows. The red particle is blind to the sites above the red dotted line.

(i) Empty sites can be pointed to and reached by a particle in a neighboring site, whereas occupied sites can be pointed to but cannot be reached.

(ii) If two or more particles point to the same site, no one of them will be allowed to reach it.

(iii) If one or more particles are pointing to a site occupied by another particle, that particle must stay at rest.

Prescription (i) is identical to mutual exclusion in sequential algorithms, and (ii) could be viewed, as usual in lattice-gas modeling, as particles attempting to reach the same site and bouncing back to their original positions. Prescription (iii) instead is something different, that can hardly be ascribed to some physical microdynamics. Since classical LGCA are constructed in such a way that the macroscopic properties arise

as a consequence of the conserved quantities and symmetries in the underlying microscopic rule, to make sure that the behavior on larger scales is actually diffusive, is a necessary step. As we will show later on, prescription (iii), besides allowing detailed balance to be preserved, does not prevent the model from exhibiting well-behaved self- and collective diffusion properties.

By means of prescriptions (ii) and (iii), *in the absence of interactions besides mutual exclusion* (which is realized by assuming that the probability of a particle to attempt a jump does not depend on the occupied site, and there are no preferred directions of motion) the transition probability matrix $\mathbf{\Omega}$ turns out to be symmetrized. In other words, if we let $n(r)$ and $n'(r)$ represent the occupancies of site r according to the configurations $\boldsymbol{\eta} = \cup_r n(r)$ and $\boldsymbol{\eta}' = \cup_r n'(r)$, respectively [mutual exclusion applies to the occupancies so that $n(r)$ can be either 0 or 1 depending on whether the site r is respectively empty or occupied], then $\Omega(\boldsymbol{\eta} \to \boldsymbol{\eta}') = \Omega(\boldsymbol{\eta}' \to \boldsymbol{\eta})$. This makes the system microcanonical and the configuration space equal to the set of all the possible arrangements of N particles in L sites.

We now translate into a formula the three prescriptions above. First of all, we need to define the neighborhood of each site, along with the particle probability to attempt a jump into a neighboring site.

Let us indicate as r (with $r \in \mathcal{L}$) a generic site of the lattice $\mathcal{L}$. Every site is connected to a finite number $\nu(r)$ (called the *connectivity* of site r) of different sites, listed in the set $\mathcal{I}(r)$ and called *neighbors of* r. In order to define $\mathcal{I}(r)$, we introduce $p(r,r')$ (with $r \neq r'$) as the probability of a lone particle, located in the site r, to attempt a jump into the site r'. Then the set of neighbors of r can be defined as $\mathcal{I}(r) := \{r' \in \mathcal{L} | p(r,r') > 0,\ r \neq r'\}$. A suitable choice for $p(r,r')$ is

$$p(r,r') = \frac{e^{\beta[\varepsilon(r) - \psi(r,r')]}}{\nu_{\max}}, \qquad r \neq r', \tag{2}$$

where $\varepsilon(r) \leqslant 0$ is the adsorption energy at the site r, the term $\psi(r,r') \geqslant 0$ [satisfying the symmetry relation $\psi(r,r') = \psi(r',r)$] is the energy barrier between the sites r and r', and $\nu_{\max} = \sup_{r \in \mathcal{L}} \nu(r)$ is the highest connectivity in the lattice. The probability $p(r,r)$ of the particle choosing not to move from where it is is defined then as

$$p(r,r) = 1 - \sum_{r' \in \mathcal{I}(r)} p(r,r'). \tag{3}$$

At each time step, at every site (independently of the other sites), say r, if the site is occupied by a particle we choose which destination site the particle can attempt a jump into. We consider $\nu(r)+1$ Booleans $\xi(r,r), \xi(r,r_1), \xi(r,r_2), \ldots, \xi(r,r_{\nu(r)})$, one for the site r itself and one for each of the neighbors of r, such that only one of those has value 1 while the others are zero, and we say that if r' is the neighbor of r for which $\xi(r,r') = 1$ then the particle will attempt a jump from r to r'. We assume a random selection criterion by picking $\xi(r,r') = 1$ with probability $p(r,r')$. Once this selection is performed at every occupied site of the lattice (the selections are independent from site to site, and thus they can be performed in parallel) on the basis of the trial directions of all the particles we apply the three acceptance criteria listed above to determine which jump attempts are to be confirmed and which ones are to be rejected (again, these operations can be performed in parallel). The evolution rule for the site occupancies reads then

$$n^{t+\tau}(r) - n^t(r) = \omega^t_{+1}(r)[1 - n^t(r)] - \omega^t_{-1}(r) n^t(r), \tag{4}$$

where t is the discrete time ($t = 0, \tau, 2\tau, \ldots$), and τ is the duration (in seconds) of a time step. The quantities ω_{+1} and ω_{-1} in Eq. (4) determine respectively the creation and the destruction of particles in the lattice sites. They depend on the configuration of the neighborhood around each site, and are structured in such a way that, for every site in which ω_{+1} created a particle, there is another site in the neighborhood of the first one where ω_{-1} destroyed another particle:

$$\begin{aligned} \omega^t_{+1}(r) &= \sum_{r' \in \mathcal{I}(r)} \xi^t(r',r) n^t(r') \chi(r, \boldsymbol{\eta}^t), \\ \omega^t_{-1}(r) &= \sum_{r' \in \mathcal{I}(r)} \xi^t(r,r') \left[1 - n^t(r')\right] \chi(r, \boldsymbol{\eta}^t), \end{aligned} \tag{5}$$

where the term $\chi(r, \boldsymbol{\eta})$, which reads

$$\begin{aligned} \chi(r, \boldsymbol{\eta}^t) = &\prod_{\substack{r'' \in \mathcal{I}(r') \\ r'' \neq r}} [1 - \xi^t(r'',r') n^t(r'')] \\ &\times \prod_{\substack{r''' \in \mathcal{I}(r) \\ r''' \neq r'}} [1 - \xi^t(r''',r) n^t(r''')], \end{aligned} \tag{6}$$

implements prescriptions (ii) and (iii) in the rule. Equations (4) to (6) will be used in Sec. IV for the derivation of the macroscopic evolution equation of nodes.

The same algorithm can be obviously cast into a form that describe the motion of N *distinguishable* particles $i = 1, \ldots, N$:

$$r_i^{t+\tau} = r_i^t + \sum_{r' \in \mathcal{I}(r)} \left(r' - r_i^t\right) \xi^t\left(r_i^t, r'\right) [1 - n^t(r')] \chi(r_i^t, \boldsymbol{\eta}^t), \tag{7}$$

acting independently, at time t, on every particle i. The evolution of the model under the representation of distinguishable particles will be used in Sec. III to derive the equilibrium distribution of configurations.

In order for detailed balance to be satisfied, we must have $\psi(r,r') = \psi(r',r)$, i.e., the absence of any kind of drift, such that the height of the barrier between two connected sites, say r_a and r_b, is the same for a particle moving from r_a to r_b or from r_b to r_a. If this is the case, then the motion of the particles will be purely diffusive and the model will converge to equilibrium; otherwise, the existence of preferred directions of motion will cause convection to add to diffusion and the system to converge to a stationary state rather than an equilibrium state. Note that if the adsorption energy ε is the same everywhere in the lattice then $\Omega(\boldsymbol{\eta} \to \boldsymbol{\eta}') = \Omega(\boldsymbol{\eta}' \to \boldsymbol{\eta})$, causing the system to be microcanonical as in the example we made above; otherwise $f(\boldsymbol{\eta})\Omega(\boldsymbol{\eta} \to \boldsymbol{\eta}') = f(\boldsymbol{\eta}')\Omega(\boldsymbol{\eta}' \to \boldsymbol{\eta})$, where $f(\boldsymbol{\eta})$ is the equilibrium probability of configuration $\boldsymbol{\eta}$ and the equilibrium state of the system will be described by the canonical ensemble statistics, as we will show in Sec. III.

III. EQUILIBRIUM DISTRIBUTION OF CONFIGURATIONS

For convenience, without loss of generality we will describe the system in terms of configurations of *distinguishable* particles $i = 1, \ldots, N$ with coordinates $\mathbf{r}^N = \{r_1, \ldots, r_N\}$. We will then consider the case of a transformation from the configuration of distinguishable particles $\mathbf{r}^N$ to $\mathbf{r}'^N$ (in short, $\mathbf{r}^N \to \mathbf{r}'^N$), that is, particle 1 moving from r_1 to r_1', particle 2 moving from r_2 to r_2', and so on. Correspondingly, the global configuration of site occupancies will change from $\boldsymbol{\eta} \to \boldsymbol{\eta}'$, i.e., occupancies will change from $n(r)$ to $n'(r)$ for every site $r \in \mathcal{L}$. Then we factorize the transition probability into two contributions, respectively from the *moving* and from the *resting* particles:

$$\Omega(\mathbf{r}^N \to \mathbf{r}'^N) = \Omega_{\mathrm{mov}}(\mathbf{r}^N \to \mathbf{r}'^N)\Omega_{\mathrm{rest}}(\mathbf{r}^N \to \mathbf{r}'^N). \quad (8)$$

Evaluation of the first term in the RHS of Eq. (8) is straightforward if we consider that if a particle, say i, is actually moving from r_i to r_i' during the transition $\mathbf{r}^N \to \mathbf{r}'^N$, then this means that when the system was described by the configuration $\mathbf{r}^N$ the site pointed at, r_i', was empty, and no other particles were pointing to it nor to r_i. Then the contribution of particle i to the transition probability is $p(r_i, r_i')$, and the transition probabilities in the two directions are

$$\Omega_{\mathrm{mov}}(\mathbf{r}^N \to \mathbf{r}'^N) = \prod_{i,\mathrm{moving}} p(r_i, r_i'), \quad (9)$$

$$\Omega_{\mathrm{mov}}(\mathbf{r}'^N \to \mathbf{r}^N) = \prod_{i,\mathrm{moving}} p(r_i', r_i). \quad (10)$$

We can obtain Eqs. (9) and (10) also through a more detailed reasoning. Let us consider again the particle i, moving from r to r' during the transformation $\mathbf{r}^N \to \mathbf{r}'^N$. We now imagine that, when the system configuration is $\mathbf{r}^N$, we choose to select the trial direction for every particle *sequentially* rather than synchronously. We stress that we do *not* imagine sequential update of the particles' position, but simply assign the trial displacements to one particle at a time. This does not change the result of the global operation, since the particles select their respective trial directions independently of each other. Now, let us assume that the last particle we invoke is particle i, so that all the $\xi(r, r')$, with $r' \in \mathcal{I}(r)$ and $r \neq r_i$, are already known. Thus, the probability of the particle to actually move from r_i to r_i' is

$$p(r_i, r_i')\overline{n}(r_i')\chi(r_i, \boldsymbol{\eta}(r_i)),$$

where $\overline{n}(\cdot)$ is a shorthand notation for $1 - n(\cdot)$. Now, since we are assuming that during the transformation $\mathbf{r}^N \to \mathbf{r}'^N$ the particle i does move from r_i to r_i', we have (1) that $n(r_i') = 0$ (i.e., the occupancy of the site targeted by i when the system is configured as $\mathbf{r}^N$) and consequently $1 - n(r_i') = 1$, and (2) that $\chi(r_i, \boldsymbol{\eta}(r_i)) = 1$. Therefore, the probability above is simplified to $p(r_i, r_i')$. The same can be done to calculate the contribution of particle i to the backward transformation $\mathbf{r}'^N \to \mathbf{r}^N$, where the particle moves from r_i' to r_i, obtaining $p(r_i', r_i)$. We could equally assume also any other particle in the system to be the last one invoked to select its trial direction, since such selections are independent from particle to particle, thus getting Eqs. (9) and (10).

We can express the resting particles' contribution to the forward transition as

$$\Omega_{\mathrm{rest}}(\mathbf{r}^N \to \mathbf{r}'^N) = \prod_{i,\mathrm{resting}} \left[p(r_i, r_i) + \sum_{r_i'' \in \mathcal{I}(r_i)}^{*} p(r_i, r_i'') \right], \quad (11)$$

where the asterisk on the summation sign indicates the following restriction: The probability $p(r_i, r_i'')$ enters the summation if the target site is such that:

(1) Due to the selection (performed by the operators $\omega_{\pm 1}$) of the allowed displacements, the position of particle i actually does not change during the transformation $\mathbf{r}^N$ to $\mathbf{r}'^N$ (otherwise, i would enter the set of moving particles instead of that of the resting particles), and if

(2) none of the effective displacements performed by the moving particles are affected by the fact that particle i chose r_i'' as target site (otherwise, such moving particles would no longer belong to the set of moving particles but they would enter the set of resting particles).

However, this is possible only if in the contributions from the resting particles there are no trial directions pointing toward neighbors whose occupancies change during the transformation. The latter condition for the site r_i'', neighbor of r_i, is $n(r_i'')n'(r_i'') + \overline{n}(r_i'')\overline{n}'(r_i'') = 1$. Therefore we can write

$$\sum_{r_i'' \in \mathcal{I}(r_i)}^{*} p(r_i, r_i'') = \sum_{r_i'' \in \mathcal{I}(r_i)} [p(r_i, r_i'')]^{n(r_i'')n'(r_i'') + \overline{n}(r_i'')\overline{n}'(r_i'')}.$$

We can do the same for the backward transition. Then one can check that $\Omega_{\mathrm{rest}}(\mathbf{r}^N \to \mathbf{r}'^N) = \Omega_{\mathrm{rest}}(\mathbf{r}'^N \to \mathbf{r}^N)$. Now we can check whether the detailed balance equation $f(\mathbf{r}^N)\Omega(\mathbf{r}^N \to \mathbf{r}'^N) = f(\mathbf{r}'^N)\Omega(\mathbf{r}'^N \to \mathbf{r}^N)$ [implying $f(\boldsymbol{\eta})\Omega(\boldsymbol{\eta} \to \boldsymbol{\eta}') = f(\boldsymbol{\eta}')\Omega(\boldsymbol{\eta}' \to \boldsymbol{\eta})$] with f as the equilibrium probability distribution of configurations, is verified:

$$f(\mathbf{r}^N) \prod_{i,\mathrm{moving}} p(r_i, r_i') = f(\mathbf{r}'^N) \prod_{i,\mathrm{moving}} p(r_i', r_i), \quad (12)$$

which can be written as

$$f(\mathbf{r}^N) \prod_{i,\mathrm{moving}} e^{\beta\varepsilon(r_i)} = f(\mathbf{r}'^N) \prod_{i,\mathrm{moving}} e^{\beta\varepsilon(r_i')}, \quad (13)$$

since $\psi(r, r') = \psi(r', r)$. Now, if we consider that, for a generic function g of the configuration,

$$\prod_{i,\mathrm{moving}} [g(r_i, \boldsymbol{\eta})] = \prod_{r \in \mathcal{L}} [g(r, \boldsymbol{\eta})]^{n(r)\overline{n}'(r)},$$

and that

$$\prod_{i,\mathrm{resting}} [g(r_i, \boldsymbol{\eta})] = \prod_{r \in \mathcal{L}} [g(r, \boldsymbol{\eta})]^{n(r)n'(r)}, \quad (14)$$

and multiply both sides of Eq. (13) by $\prod_r [e^{\beta\varepsilon(r)}]^{n(r)n'(r)}$, we can switch from the distinguishable to the indistinguishable particle representation:

$$f(\boldsymbol{\eta}) \prod_{r \in \mathcal{L}} e^{\beta n(r)\varepsilon(r)} = f(\boldsymbol{\eta}') \prod_{r \in \mathcal{L}} e^{\beta n'(r)\varepsilon(r)}. \quad (15)$$

Thus the detailed balance relation is verified if the equilibrium distribution of the model has the form

$$f(\boldsymbol{\eta}) \propto \prod_{r \in \mathcal{L}} e^{-\beta n(r)\varepsilon(r)}. \quad (16)$$

If we put the RHS of the relation (16) in the form of $e^{-\beta\mathcal{H}(\boldsymbol{\eta})}$, where $\mathcal{H}(\boldsymbol{\eta})$ is the lattice Hamiltonian, we get

$$\mathcal{H}(\boldsymbol{\eta}) = \sum_r n(r)\varepsilon(r). \tag{17}$$

IV. DIFFUSIVE BEHAVIOR

Once we know the form of the equilibrium distribution, we want to check whether the prescriptions inserted in the rule to make it fully parallel without creating any conflict with mutual exclusion and detailed balance cause the diffusion to be either normal or anomalous. We do it through inspection of the behavior of relevant time-correlation functions calculated over data obtained from numerical simulations, and through simple theoretical considerations over several one- and two-dimensional test systems. We anticipate that although the evolution rule is derived from a glass-forming algorithm and the prescriptions necessary to achieve the full synchronicity of the rule (especially the third one) are particularly strict, in all the numerical simulations we perform to test the model we will find both the single-particle motion and the motion of the center of mass to be normally diffusive.

The test systems are constructed by replicating along the available directions a unit cell made of P and Q sites, characterized respectively by the adsorption energy ε_P and ε_Q and arranged differently from system to system. Since our aim was to study the isotropic diffusion of particles *at equilibrium* (i.e., without convection), we chose the symmetric arrangements sketched in Fig. 2. According to Fig. 2, from now on we will refer to such systems as (a), (b), (c), and (d), respectively.

For theoretical arguments, the systems were supposed to be infinite. For numerical simulations, periodic boundary conditions were applied.

The physical time step duration τ is assumed to be the same for all the simulations, as well as constant throughout each simulation. For the purpose of the present study, which is to assess the suitability of our evolution rule as a diffusion rule, there is no need to assign it an explicit value. However, any future application of the model would require an explicit connection between τ and some characteristic time extracted from experiments or atomistic simulation over the system investigated [18].

A. Macroscopic equations

It is usual in the presentation of CA algorithms to derive, under convenient simplifying assumptions, the macroscopic equations governing some relevant local observables, e.g., the local density [1]. The problem to deal with in such derivations is represented by the noise introduced by correlations in space and time [1,19–21]. CA evolution rules are discrete, and therefore the evolution of such systems is noisy by default. In practice, the noise in CA trajectories can be mitigated by averaging the occupancies over relatively large portions of a very large system (and in time as well) [1,8], making possible the definition of a proper "local density," or by relaxing the exclusion principle, thus allowing an arbitrary number of particles to occupy the same site [1,22]. Theoretically, if the CA rule is very simple one can attempt to derive the macroscopic evolution equations by writing the rule in the form of a discrete master equation, and then associating a continuous field with it and using the concepts of field theory to obtain an equation equipped with noise terms. The procedure is technically complex, and applying it to the analysis of complicated rules can turn out to be a difficult task. Assumptions like the Boltzmann chaos hypothesis and the slowly varying density in space and/or time are often made to simplify the problem. Although simplifying assumptions can lead to erroneous results, they are of help in the first stage of construction of a CA rule since they allow the realization that, even though correlations are discarded (either totally or partially), the macroscopic behavior thus derived at least *formally* resembles the one we wish it had (a diffusion equation in this case). In such a case, one can proceed with a more detailed statistical analysis of the trajectories obtained through numerical simulation to check whether they show a normal diffusion behavior.

This is exactly the route we follow to assess the diffusion behavior of the present model. Strong correlations are expected, due to the fact that (i) an exclusion principle holds, (ii) prescriptions are introduced that prevent a particle from moving depending on the configuration of the trial displacement of the particles in its neighborhood, and (iii) many terms are involved in Eqs. (4) to (6), from the first as well as from the second neighborhood of a site. Therefore, as usual in the derivation of macroscopic equations from the microscopic evolution rules of cellular automata [1], some simplifying assumptions are needed as necessary technical steps to get from *micro* to *macro*, even though it could turn out to be quite difficult to rigorously prove their validity.

We will derive the formal macroscopic equation for our evolution rule applied to the case of a square lattice [system (b) of Fig. 2], where a particle can point toward its first neighbors only. The same steps can be straightforwardly applied to the one- and the three-dimensional cases to get analogous results.

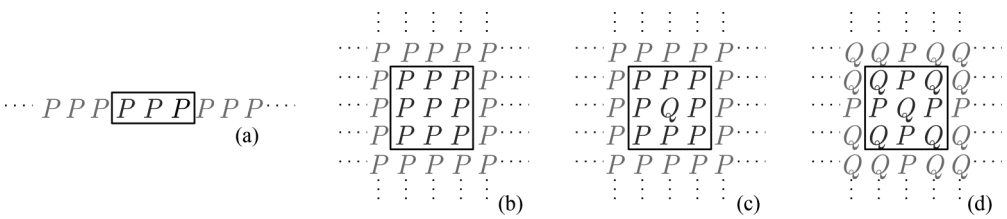

FIG. 2. Sketch of four systems we describe in the paper. In each subfigure, the sites constituting the unit cell, repeating in one dimension for the system in (a) and in two dimensions in (b), (c), and (d), are enclosed within a rectangle.

The lattice is assumed homogeneous and of infinite size. The evolution of the occupancy of the site of coordinates (x,y) depends on the occupation and trial direction at sites $\{(x+q\lambda, y+w\lambda)|q,w=-2,\dots,2\}$. The state of the system is assumed to fluctuate dynamically around the equilibrium state by which it is described in the long-time limit.

We represent the four directions of motion as $\leftarrow$, $\rightarrow$, $\downarrow$, and $\uparrow$. The change in the occupancy of site (x,y) during one time step (of duration τ) is

$$\Delta_\tau n_{x,y} = \Delta_\tau n^{\rightarrow}_{x,y} + \Delta_\tau n^{\leftarrow}_{x,y} + \Delta_\tau n^{\uparrow}_{x,y} + \Delta_\tau n^{\downarrow}_{x,y}, \quad (18)$$

where $\Delta_\tau n^{\rightarrow}_{x,y}$ is the contribution to the occupation change of (x,y) coming from the exchange with $(x+\lambda,y)$, $\Delta_\tau n^{\leftarrow}_{x,y}$ is the contribution to the occupation change of (x,y) coming from the exchange with $(x-\lambda,y)$, and so on:

$$\begin{aligned}\Delta_\tau n^{\rightarrow}_{x,y} = {} & [(1-n_{x,y})n_{x+\lambda,y}\xi^{\leftarrow}_{x+\lambda,y} - n_{x,y}\xi^{\rightarrow}_{x,y}(1-n_{x+\lambda,y})] \\ & \times(1-n_{x+2\lambda,y}\xi^{\leftarrow}_{x+2\lambda,y})(1-n_{x+\lambda,y+\lambda}\xi^{\downarrow}_{x+\lambda,y+\lambda}) \\ & \times(1-n_{x+\lambda,y-\lambda}\xi^{\uparrow}_{x+\lambda,y-\lambda})(1-n_{x-\lambda,y}\xi^{\rightarrow}_{x-\lambda,y}) \\ & \times(1-n_{x,y+\lambda}\xi^{\downarrow}_{x,y+\lambda})(1-n_{x,y-\lambda}\xi^{\uparrow}_{x,y-\lambda}), \end{aligned} \quad (19)$$

$$\begin{aligned}\Delta_\tau n^{\leftarrow}_{x,y} = {} & [(1-n_{x,y})n_{x-\lambda,y}\xi^{\rightarrow}_{x-\lambda,y} - n_{x,y}\xi^{\leftarrow}_{x,y}(1-n_{x-\lambda,y})] \\ & \times(1-n_{x-2\lambda,y}\xi^{\rightarrow}_{x-2\lambda,y})(1-n_{x-\lambda,y+\lambda}\xi^{\downarrow}_{x-\lambda,y+\lambda}) \\ & \times(1-n_{x-\lambda,y-\lambda}\xi^{\uparrow}_{x-\lambda,y-\lambda})(1-n_{x+\lambda,y}\xi^{\leftarrow}_{x+\lambda,y}) \\ & \times(1-n_{x,y+\lambda}\xi^{\downarrow}_{x,y+\lambda})(1-n_{x,y-\lambda}\xi^{\uparrow}_{x,y-\lambda}), \end{aligned} \quad (20)$$

$$\begin{aligned}\Delta_\tau n^{\uparrow}_{x,y} = {} & [(1-n_{x,y})n_{x,y+\lambda}\xi^{\downarrow}_{x,y+\lambda} - n_{x,y}\xi^{\uparrow}_{x,y}(1-n_{x,y+\lambda})] \\ & \times(1-n_{x+\lambda,y+\lambda}\xi^{\leftarrow}_{x+\lambda,y+\lambda})(1-n_{x-\lambda,y+\lambda}\xi^{\rightarrow}_{x-\lambda,y+\lambda}) \\ & \times(1-n_{x,y+2\lambda}\xi^{\downarrow}_{x,y+2\lambda})(1-n_{x+\lambda,y}\xi^{\leftarrow}_{x+\lambda,y}) \\ & \times(1-n_{x-\lambda,y}\xi^{\rightarrow}_{x-\lambda,y})(1-n_{x,y-\lambda}\xi^{\uparrow}_{x,y-\lambda}), \end{aligned} \quad (21)$$

$$\begin{aligned}\Delta_\tau n^{\downarrow}_{x,y} = {} & [(1-n_{x,y})n_{x,y-\lambda}\xi^{\uparrow}_{x,y-\lambda} - n_{x,y}\xi^{\downarrow}_{x,y}(1-n_{x,y-\lambda})] \\ & \times(1-n_{x+\lambda,y-\lambda}\xi^{\leftarrow}_{x+\lambda,y-\lambda})(1-n_{x-\lambda,y-\lambda}\xi^{\rightarrow}_{x-\lambda,y-\lambda}) \\ & \times(1-n_{x,y-2\lambda}\xi^{\uparrow}_{x,y-2\lambda})(1-n_{x+\lambda,y}\xi^{\leftarrow}_{x+\lambda,y}) \\ & \times(1-n_{x-\lambda,y}\xi^{\rightarrow}_{x-\lambda,y})(1-n_{x,y+\lambda}\xi^{\downarrow}_{x,y+\lambda}). \end{aligned} \quad (22)$$

We dropped the time superscript t for better readability. Now, since the Boolean $\xi^{\circ}_{x+q\lambda,y+w\lambda}$ (with $\circ = \rightarrow, \leftarrow, \uparrow, \downarrow$) is picked randomly at every site $(x+q\lambda, y+w\lambda)$, its ensemble average corresponds to the following probabilities:

$$\begin{aligned}\langle\xi^{\leftarrow}_{x+q\lambda,y+w\lambda}\rangle = \langle\xi^{\rightarrow}_{x+q\lambda,y+w\lambda}\rangle = \tfrac{1}{4}e^{-\beta\psi_x}e^{\beta\varepsilon}, \\ \langle\xi^{\downarrow}_{x+q\lambda,y+w\lambda}\rangle = \langle\xi^{\uparrow}_{x+q\lambda,y+w\lambda}\rangle = \tfrac{1}{4}e^{-\beta\psi_y}e^{\beta\varepsilon}, \end{aligned} \quad (23)$$

where q and w are integers in the interval $-2 \leqslant q,w \leqslant 2$, ε is the site adsorption energy, and $\psi_x, \psi_y \geqslant 0$ are migration barriers along the x and the y directions, respectively. We then average both sides of Eq. (18) over an ensemble of equivalent systems [1] to get

$$\begin{aligned}\langle\Delta_\tau n_{x,y}\rangle = {} & \tfrac{1}{4}e^{\beta\varepsilon}\{-\langle n_{x,y}\rangle(2e^{-\beta\psi_x}+2e^{-\beta\psi_y}) \\ & + e^{-\beta\psi_x}[\langle n_{x+\lambda,y}\rangle + \langle n_{x-\lambda,y}\rangle] + e^{-\beta\psi_y}[\langle n_{x,y+\lambda}\rangle \\ & + \langle n_{x,y-\lambda}\rangle] + C_1 e^{-\beta\psi_x} + C_2 e^{-\beta\psi_y} + \cdots\}, \end{aligned} \quad (24)$$

where the coefficients $C_1, C_2, \dots$ are sums of several two- up to seven-body static correlation functions of the form $\langle n_{x_1,y_1} n_{x_2,y_2} \cdots n_{x_k,y_k} \cdots \rangle$. Due to the very large number of terms, we do not report formulas for them. We neglect time correlations. We further assume that local densities fluctuate closely around stationarity, and that a general symmetry criterion holds such that the correlation between two nodes r_a and r_b depends only on their distance $|r_a - r_b|$, and similarly for the correlation among three nodes and more: Let us consider two different sets of sites $A = \{u_1, \dots, u_K\}$ and $B = \{v_1, \dots, v_K\}$. For a square lattice, the coordinates of site u_1 are (u_{1x}, u_{1y}), the coordinates of site u_2 are (u_{2x}, u_{2y}), and so on, and similarly for sites v_1, v_2, etc. For the sake of clarity, with a slight temporary change in notation we let $n(u_1)$ be the occupation state of site u_1, $n(u_2)$ the occupation state of u_2, and so on. Now we indicate as

$$\langle n_A\rangle = \left\langle \prod_{k=1}^{K} n(u_k) \right\rangle \quad \text{and} \quad \langle n_B\rangle = \left\langle \prod_{k=1}^{K} n(v_k) \right\rangle \quad (25)$$

the static correlation functions involving the sets of sites A and B. We then construct the two sets $\mathcal{S}_A$ and $\mathcal{S}_B$, given by the collection of the absolute distances between all the different site pairs obtainable from sets A and B, respectively:

$$\mathcal{S}_A = \bigcup_{k=1}^{K-1} \bigcup_{k'=k+1}^{K} |u_k - u_{k'}|, \quad \mathcal{S}_B = \bigcup_{k=1}^{K-1} \bigcup_{k'=k+1}^{K} |v_k - v_{k'}|. \quad (26)$$

Since ψ_x and ψ_y do not vary from site to site, if $\mathcal{S}_A = \mathcal{S}_B$ then also $\langle n_A\rangle = \langle n_B\rangle$. We put $\langle n_{i,j}\rangle = \rho$ and Taylor expand the terms in the RHS of Eq. (24):

$$\begin{aligned}\langle n_{i\pm1,j}\rangle &= \rho \pm \lambda\partial_x\rho + \frac{\lambda^2}{2}\partial_x^2\rho + O(\lambda^3), \\ \langle n_{i,j\pm1}\rangle &= \rho \pm \lambda\partial_y\rho + \frac{\lambda^2}{2}\partial_y^2\rho + O(\lambda^3), \end{aligned} \quad (27)$$

to get

$$\begin{aligned}& \tau\partial_t\rho + \frac{\tau^2}{2}\partial_t^2\rho + O(\tau^3) \\ & \quad = \frac{\lambda^2}{4}e^{\beta\varepsilon}\left\{e^{-\beta\psi_x}\partial_x^2\rho + e^{-\beta\psi_y}\partial_y^2\rho\right\} + O(\lambda^3). \end{aligned} \quad (28)$$

Now, as usual in a diffusion process [1], we take the limit $\lambda \to 0, \tau \to 0$ with $\lambda^2/\tau \to$ const to get the diffusion equation

$$\partial_t\rho = D_x\partial_x^2\rho + D_y\partial_y^2\rho, \quad (29)$$

where

$$D_x = \frac{\lambda^2}{4\tau}e^{\beta(\varepsilon-\psi_x)}, \qquad D_y = \frac{\lambda^2}{4\tau}e^{\beta(\varepsilon-\psi_y)} \quad (30)$$

are Fickian diffusivities in the two directions of motion.

As we can see, once we assume correlations to be distance dependent, we obtain that the multibody correlation terms cancel out, providing the same result we would obtain by simply neglecting the noise terms $C_1, C_2, \dots$ in Eq. (24). As a result, mutual exclusion and correlations do not enter the macroscopic equation, and the Fickian diffusion coefficients turn out to be simply proportional to the ability of the particle to move along the respective directions.

Although in Eqs. (29) and (30) the lattice directions are made "visible" by the fact that $\psi_x - \psi_y \neq 0$ [1], still the relation $\psi(r,r') = \psi(r',r)$ holds, so that in the long-time limit the system will fluctuate around the same equilibrium state described by the lattice Hamiltonian (17). If we put $\psi = \psi_x = \psi_y$, then the mobilities are simply rescaled and we get $\partial_t \rho = D\nabla^2 \rho$, with a diffusion coefficient

$$D = \frac{\lambda^2}{4\tau} e^{\beta(\varepsilon - \psi)}. \tag{31}$$

Similar results are found for heterogeneous lattices. Let us consider the system with unit cells sketched in Figs. 2(c) and 2(d), with infinite size and homogeneous site-to-site barrier ψ. To get the macroscopic evolution equation of the local densities as we did for the previous case, analogously to Eq. (18) we write down the evolution equation for the discrete occupancy rates $\Delta_\tau n_{x,y}$ (the site at the center of the unit cell), $\Delta_\tau n_{x+\lambda,y}$, $\Delta_\tau n_{x,y-\lambda}$, $\Delta_\tau n_{x-\lambda,y}$, $\Delta_\tau n_{x,y+\lambda}$ (the rates at the first neighbors), and $\Delta_\tau n_{x+\lambda,y+\lambda}$, $\Delta_\tau n_{x+\lambda,y-\lambda}$, $\Delta_\tau n_{x-\lambda,y-\lambda}$, $\Delta_\tau n_{x-\lambda,y+\lambda}$ (the rates at the second neighbors within the same unit cell). Now the quantities $\langle \xi^{\circ}_{x+q\lambda,y+w\lambda} \rangle$ are no longer site independent, since the adsorption energy can be either ε_P or ε_Q depending on the site. We sum up those equations, and again we assume that $\langle n_A \rangle = \langle n_B \rangle$ if $\mathcal{S}_A = \mathcal{S}_B$ but this time we need to slightly modify the formulas in (26) to take account of the heterogeneity of the sites. Our choice is

$$\begin{aligned} \mathcal{S}_A &= \bigcup_{k=1}^{K-1} \bigcup_{k'=k+1}^{K} w(u_k) w(u'_k) |u_k - u_{k'}|, \\ \mathcal{S}_B &= \bigcup_{k=1}^{K-1} \bigcup_{k'=k+1}^{K} w(v_k) w(v'_k) |v_k - v_{k'}|, \end{aligned} \tag{32}$$

where the $w(\cdot)$'s are arbitrary weights assigned to the sites in such a way that all the P sites have the same weight, say w_P, all the Q sites have the weight w_Q, and $w_P \neq w_Q$. We obtain a diffusion equation where the diffusivity has the following form:

$$D = \frac{\lambda^2}{\tau} \frac{f_P \rho_P P + f_Q \rho_Q Q}{K\rho}, \tag{33}$$

where $P = \frac{1}{4} e^{\beta(\varepsilon_P - \psi)}$ and $Q = \frac{1}{4} e^{\beta(\varepsilon_Q - \psi)}$ represent the escape probabilities of a free particle from a P and a Q site, respectively, K is the total number of sites in one unit cell, and ρ_P and ρ_Q are respectively the average occupancies of a P and of a Q site, satisfying the relation

$$K_P \rho_P + K_Q \rho_Q = K\rho,$$

with K_P and K_Q as the numbers of P and Q sites in one unit cell, respectively, for which $K_P + K_Q = K$. Moreover, since there are no site-site interactions other than mutual exclusion, due to the lattice Hamiltonian (17) ρ_P and ρ_Q obey Fermi-Dirac statistics, so that $\rho_X = e^{\beta(\mu - \varepsilon_X)}/[1 + e^{\beta(\mu - \varepsilon_X)}]$, where $X = P, Q$ and μ is the chemical potential. Finally, f_P and f_Q denote respectively the numbers of P and of Q sites of a unit cell at the interface with one of the (in this case, four) neighboring cells. In the case of the system of Fig. 2(c), $f_P = 3$, $f_Q = 0$, and $K = 9$ so that $D = \frac{\lambda^2}{3\tau} P(\rho_P/\rho)$. For a unit cell like the one sketched in Fig. 2(d), instead, $f_P = 1$, $f_Q = 2$, and $K = 9$ so that $D = \frac{\lambda^2}{9\tau}[P(\rho_P/\rho) + 2Q(\rho_Q/\rho)]$.

The only relevant quantities in the macroscopic diffusivity of Eq. (33) are the relative site densities and the fraction of sites of each type at the interface with neighboring cells. Similarly to the case of homogeneous lattices, Eq. (33) contains neither mutual exclusion nor correlation terms. However, as we can see from Eq. (33), heterogeneity causes macroscopic diffusivity to depend on both concentration and temperature, whereas the Fickian diffusivity in Eq. (31), referring to a homogeneous lattice, shows only a dependence on temperature.

B. Numerical simulations

Once we found that the macroscopic equations for the local density, although derived formally neglecting the noise terms, take the form of diffusion equations, we proceeded with the investigation of the basic properties related to the particle mobility to check whether the rule prescriptions lead to anomalies in the diffusion process or not. We first provide the necessary technical details of the simulations.

The system sizes were chosen as $L = 10^4$ sites for the one-dimensional systems and $L = 90 \times 90$ sites for the two-dimensional grids. Such sizes were chosen after verifying that, with $L \geqslant 40$, the size effect on diffusion is negligible in the case of a homogeneous lattice (which, as we will show in this section, is the most sensitive to the rule prescriptions). This size is more than doubled in order to ensure a good statistical accuracy.

We set the adsorption energies to the values $\varepsilon_P = 0$ and $\varepsilon_Q = -10$ kJ mol^{-1}, and the temperature T to 300 K. The starting configuration of each simulation is chosen randomly with uniform probability over all the possible configurations in the system (i.e., as if the sites were all equivalent). This means that homogeneous lattices required no equilibration steps, whereas heterogeneous lattices required an equilibration period that we set to 10^5 steps before starting with the production of a statistical trajectory in the configuration space. For both homo- and heterogeneous systems the simulations were 10^8 time steps long. We computed the mean-square displacement (MSD) of the single-particle motion, denoted $\sigma^2(t) = \langle |r_i^t - r_i^0|^2 \rangle$, and the self-propagator, i.e., the self-part of the van Hove correlation function $P(\Delta r, t) = \langle \delta(\Delta r - r_i^t + r_i^0) \rangle$ [where $\delta(\cdot)$ is the delta function], giving the probability of finding a particle around a distance vector r at time t, given that the same particle was at the origin at time $t = 0$. We report the propagator along the x direction in Fig. 3 for several densities after 10^4 time steps (the histogram bins have size 3λ, i.e., the side of the unit cell), whereas the MSDs up to 10^6 steps are reported in Fig. 4. For all the systems we studied, the propagator along each direction of motion was well fitted by a Gaussian distribution with zero mean and variance equal to the mean-square displacement $\sigma^2(t)$ (reported in Fig. 3). As expected, the MSDs of the one-dimensional systems with $N > 1$ were all subdiffusive, since $\sigma^2(t) \sim \sqrt{t}$, a typical result of single-file diffusion (see Ref. [23] and references therein). In the long-time limit, the MSD of two-dimensional systems shows a linear time dependence. The fits (dotted lines) are shown in Fig. 4 together with simulation data (solid lines). Slower-diffusing systems take longer to reach the linear

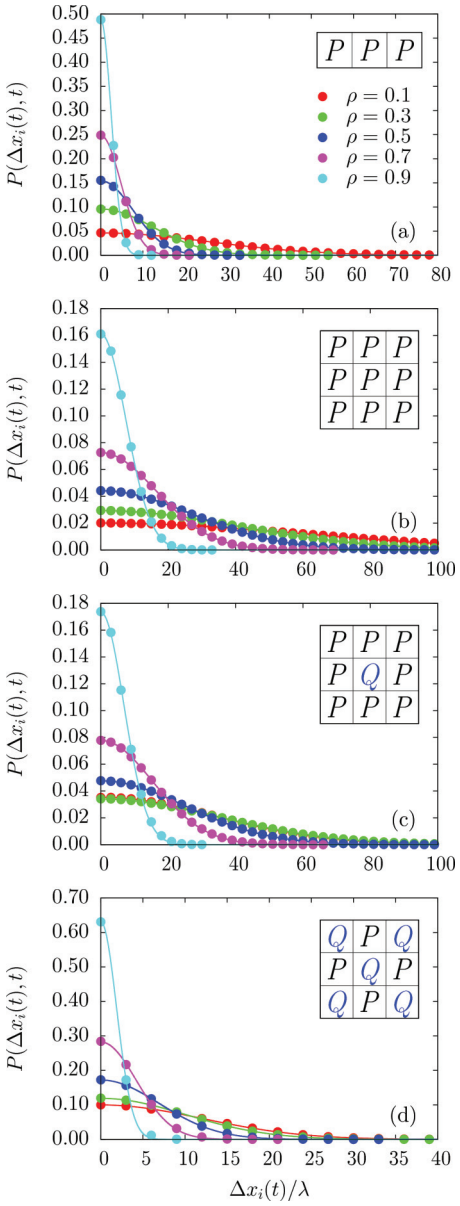

FIG. 3. (Color online) The propagator of the single-particle motion along the x coordinate at time $t = 10^4\tau$ for several two-dimensional systems. In the inset of each plot the unit cell of each system is reported, with P and Q referring to the different binding energies $\varepsilon_P = 0$ and $\varepsilon_Q = -10$ kJ mol^{-1}. The dots are simulation data, and the lines are Gaussian propagators related to the mean-square displacement value along the x coordinate.

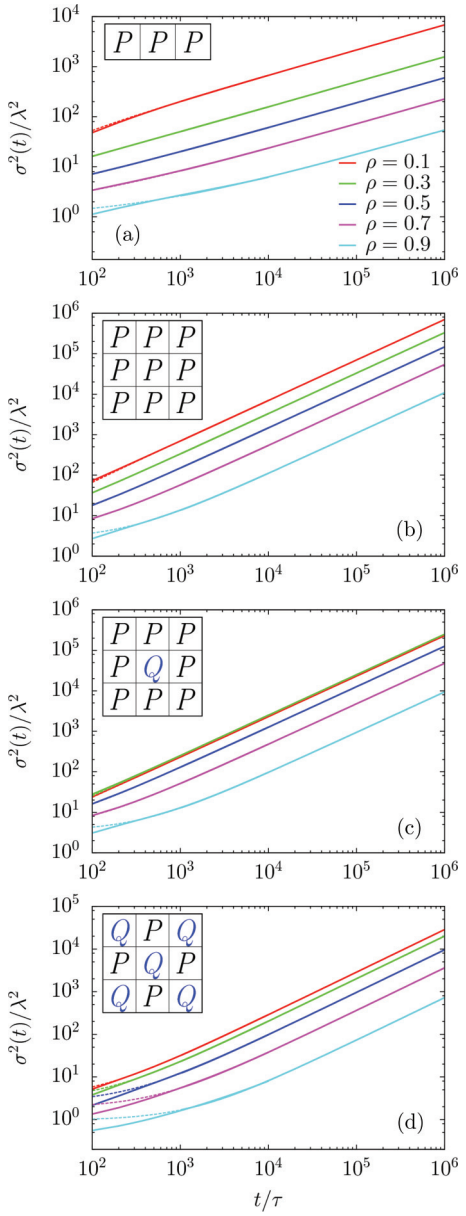

FIG. 4. (Color online) Mean-square displacement plots for the same systems reported in Fig. 3 at various densities. The solid lines are simulation data, and the dotted lines are linear ($y \sim ax$) fits for the two-dimensional systems and square fits ($y \sim a\sqrt{x}$) for the one-dimensional case (top).

regime. For example, in Fig. 4 we can see that system (d) takes a time to reach the linear regime which is about one order of magnitude larger than for systems (b) and (c), since two of the three interfacial sites of the unit cell (d), having adsorption energy ε_Q, are more binding than the other ones, whereas in the unit cells of (b) and (c) only sites with zero adsorption energy are present at the interface.

The collective motion has been studied as well, by estimating the propagator and mean-square displacement $\sigma_c^2(t)$ of the collective coordinate $r_c^t = \sum_i r_i^t$. In the cases we studied, the collective MSDs were all linear in the long-time regime (not shown) also for the one-dimensional case (this is also typical of single-file systems) and the collective propagators were again Gaussian with zero mean and variance $\sigma_c^2(t)$. No anomalies were found in the self-intermediate scattering functions (SISFs) $f_s(q,t) = \langle \exp\{iq \cdot [r_i^t - r_i^0]\}\rangle$, where $q = (2\pi n_x/L, 2\pi n_y/L)$ with $n_{x,y}$ integer. In Fig. 5 we consider the SISF for the wave vector $q = (2(L-1)\pi/L, 0)$ for systems (b), (c), and (d). In all our study cases, the SISF was well fitted by a single exponential function, i.e., $f_s(q,t) \sim \exp(-t/\tau_{\rm rel})$, where $\tau_{\rm rel}$ is the relaxation time of the system. In Fig. 5 the quantity under consideration is the product $\tau_{\rm rel} D_s$, which is of interest since the structural relaxation time scales as viscosity [24,25]. The constant trend of $\tau_{\rm rel} D_s$ indicates that the Stokes-Einstein relation is satisfied throughout the

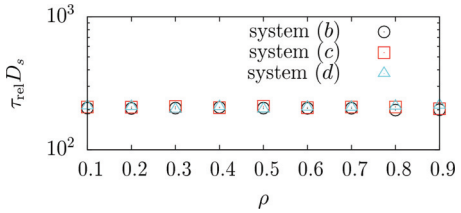

FIG. 5. (Color online) Self- and collective diffusivity plots for the same systems reported in Fig. 3. In the case of the one-dimensional system (top), due to the nonlinearity of the MSD of the single-particle motion, its slope is expressed in term of mobility F_s rather than self-diffusivity.

whole density domain $0 < \rho < 1$ [26], meaning that the rule prescriptions cause no dynamical transition, i.e., no critical density lower than the maximal density exists at which a structural arrest occurs. With all such evidence we conclude that the systems we investigated show no glassy behavior.

The self- and collective diffusion coefficients D_s (replaced by the mobility F_s in the case of the single-file system) and D_c, derived from the slopes of the MSDs, are reported in Fig. 6 as functions of the density ρ. As expected, the back-correlation effect by which a particle, once it has jumped into a new site, is more likely to jump back to the site it came from [27–29] is less evident in the collective motion, giving $D_c \geqslant D_s$. The interesting point is the curvature of the D_s plot of the homogeneous system (b). In the ideal scenario proposed by Reed and Erlich [30], in a homogeneous lattice system with low or no correlations the diffusivity should decrease linearly with the density. Standard LGCA diffusion rules [1,8], where the current configuration of particles in each cell is randomized at each time step, destroying the correlations, behave in that way when particles are subjected to the further restraint of not crossing each other when moving from cell to cell [31]. In the present case instead, no cell randomization occurs at all and the limitations to the particle movements imposed by the rule prescriptions cause memory of the previous configurations to be conserved longer. As a consequence, the reported diffusivity trend is very far from the linearly decreasing D_s vs ρ plot that we would have in the case of uncorrelated motion. It is therefore interesting to compare the diffusion properties produced by the synchronous rule with the ones obtained by means of standard MC simulations where particles move along the lattice sites through Arrhenius jumps [32]. This is done in Fig. 7, where the relative discrepancies $F_s/F_s^{\mathrm{MC}} - 1$ (for the single-file system), $D_s/D_s^{\mathrm{MC}} - 1$, and $D_c/D_c^{\mathrm{MC}} - 1$ are reported. It can be seen clearly that discrepancies are low at low densities and increase with it, until particle mobilities become less than half of the MC values at very high densities. This is an expected trend. Let us take for example the homogeneous case, system (b) in Fig. 7. Under a mean-field approximation, neglecting the back-correlation contribution, the probability of a particle leaving its current adsorption site during a time step can be estimated as $P_{\mathrm{esc}} = (1 - \rho\frac{e^{\beta\varepsilon}}{\nu})^{2(\nu-1)}(1-\rho)e^{\beta\varepsilon}$, whereas the corresponding MC quantity is $P_{\mathrm{esc}}^{\mathrm{MC}} = (1-\rho)e^{\beta\varepsilon}$. The relative discrepancy on this measure is thus

$$P_{\mathrm{esc}}/P_{\mathrm{esc}}^{\mathrm{MC}} - 1 = \left(1 - \rho\frac{e^{\beta\varepsilon}}{\nu}\right)^{2(\nu-1)}, \qquad (34)$$

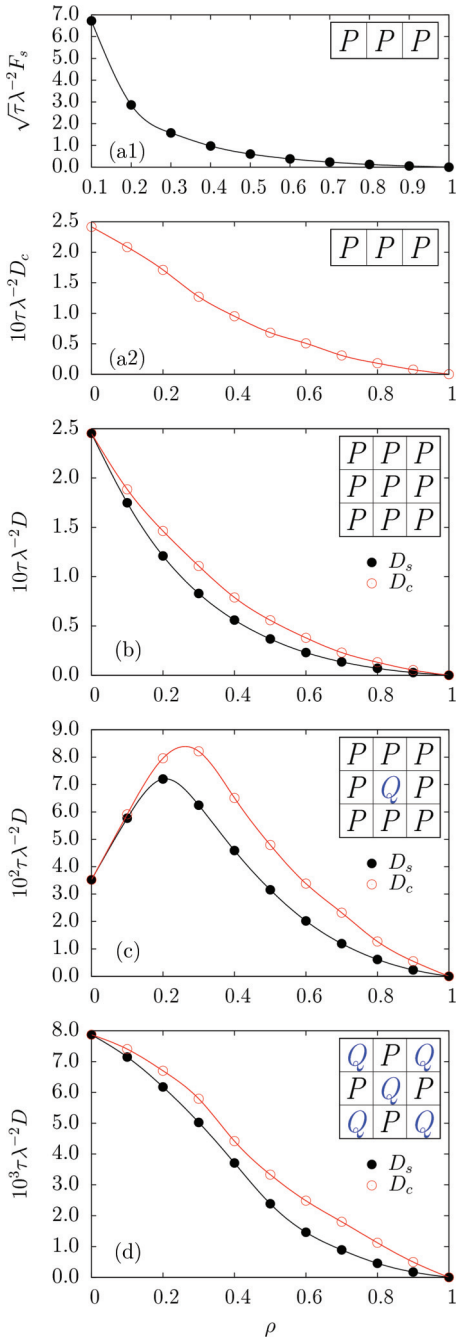

FIG. 6. (Color online) The product $\tau_{\mathrm{rel}}D_s$, where the relaxation time τ_{rel} is taken from the exponential fit of the self-intermediate scattering function for wave vector $q = (2(L-1)\pi/L, 0)$, for the systems (b), (c), and (d) reported in Fig. 3.

which becomes more negative on increasing ν and/or on making $\beta\varepsilon$ closer to zero. As a function of ρ, the shape of its decay is the same as that of system (b) in Fig. 7.

Unit cells of systems (c) and (d) instead are made of different arrangements of P and Q sites. Hence, since the escape probability is heterogeneous the shape of $D_s/D_s^{\mathrm{MC}} - 1$ vs ρ is expected to change from the homogeneous case, although still decreasing. In particular, for low densities the particles will occupy Q sites most of the time. Since the Q sites are more binding, the overall escape probability will be

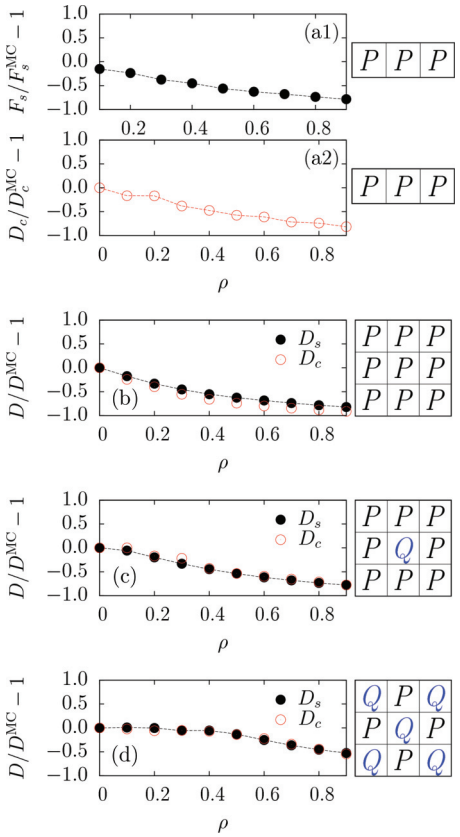

FIG. 7. (Color online) Comparison between synchronous and serial (MC) simulations of self- and collective diffusivities. The systems are the same as reported in Fig. 3.

more affected by the adsorption energy ε_Q than by the rule prescriptions. In the case of system (d) (bottom of Fig. 7), 5/9 of the sites are Q sites, thus making the effect more evident.

Therefore, our expectation is that for lattices with strong adsorption energies the diffusivities obtained with the synchronous and with the sequential MC evolutions will be similar. The confirmation of such expectation is shown in Fig. 8, where we see that when the adsorption energy of the homogeneous systems is set to -10 kJ mol^{-1} rather than 0, mutual exclusion and the adsorption energy play the most important role whereas the rule prescriptions produce a negligible effect.

C. Diffusion on a (100) fcc surface

We performed simulations of the (100) surface of a fcc crystal (see Fig. 9) with generic lattice spacing λ where two kinds of sites can be distinguished, i.e., fourfold hollow sites, named A sites, with adsorption energy ε_A (squares in Fig. 9), and twofold bridge sites, named B sites, with adsorption energy ε_B (circles in Fig. 9). Although lateral interactions are not included, besides the theoretical interest this model is adequate for the study of low-coverage layers and adatoms with weak interactions such as N on Ru(001) [33].

We compared the self-diffusion isotherms at $T = 300$ K obtained by the synchronous rule with those we get by means of a MC sequence of Arrhenius jumps. The connectivities are set as in the work of Chvoj *et al.* [34,35] (see Fig. 9), i.e.,

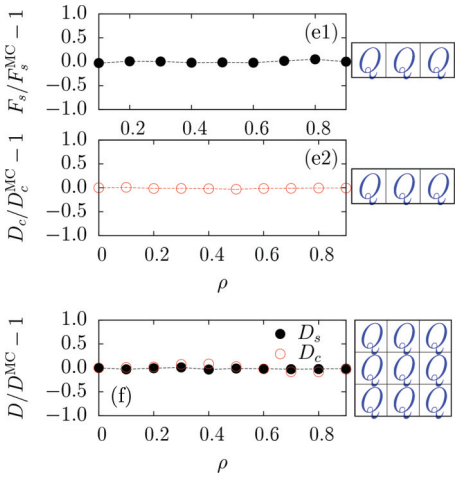

FIG. 8. (Color online) Comparison between synchronous and serial (MC) simulations of self- and collective diffusivities for two homogeneous lattices of sites having a more negative binding energy, i.e., $\varepsilon_Q = -10$ kJ mol^{-1}.

an A site leads to four B sites [in the directions $(\lambda,0)$, $(0,\lambda)$, $(-\lambda,0)$, and $(0,-\lambda)$] through a barrier ψ_{AB}, whereas a B site leads to four B sites [in the directions (λ,λ), $(-\lambda,\lambda)$, $(-\lambda,-\lambda)$, and $(\lambda,-\lambda)$] through a barrier ψ_{BB} and to two A sites [in the directions $(0,\lambda)$ and $(0,-\lambda)$ for half of the B sites and $(\lambda,0)$ and $(-\lambda,0)$ for the other half] through a barrier $\psi_{BA} = \psi_{AB}$. Simulations were carried out for square lattice boxes of size $80 \times 80\lambda^2$ containing 4800 sites, for a total of 10^6 steps after equilibration.

We first investigated two cases with $\psi_{BA} = \psi_{AB} = \psi_{BB} = 0.$, reported in Fig. 10. In the first one, indicated as fcc-a, the hollow site is deeper than the bridge site ($\varepsilon_A = -10$ kJ mol^{-1} and $\varepsilon_B = 0$). As we can see in Fig. 10 (top left) this causes particles to remain confined within the hollow sites until they reach sufficient energy to jump into the bridge sites, from which they can escape faster. Since in such a case not only are the bridge sites less binding than the hollow sites, but also they are connected to other bridge sites, we can say that mobility from a bridge site is higher. Increasing the overall density causes the average occupancy of bridge sites to increase as the number of available hollow sites decreases; therefore the particle mobility increases as well up to a maximum at

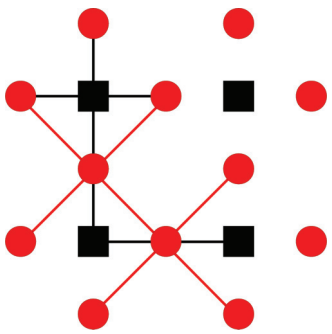

FIG. 9. (Color online) Lattice topology for the model of the (100) fcc surface. The black squares represent hollow sites (A sites) with adsorption energy ε_A, and the red circles are bridge sites with adsorption energy ε_B.

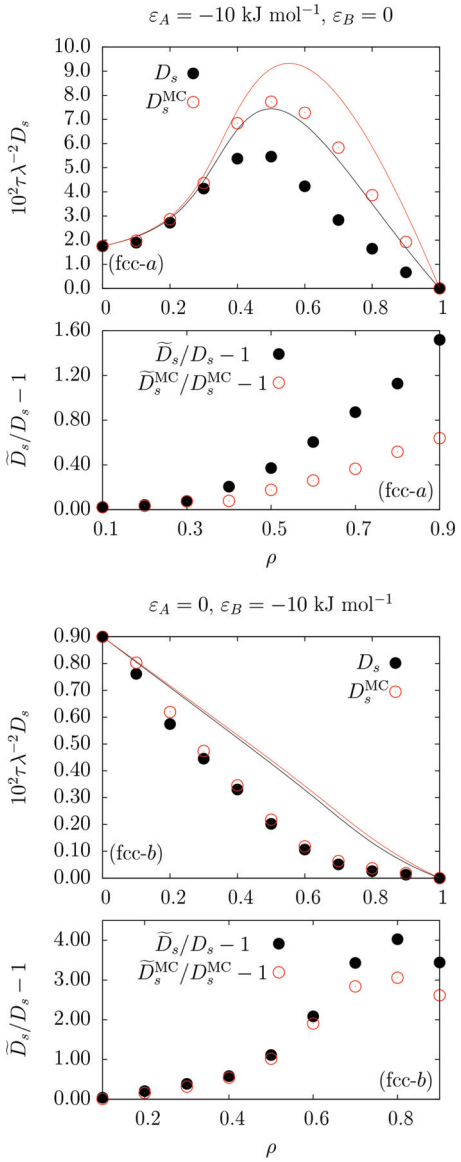

FIG. 10. (Color online) Self-diffusion profiles in the (100) fcc surface sketched in Fig. 9 at 300 K for two different configurations of the adsorption energies, together with the relative discrepancy between the numerical and the mean-field values of the self-diffusivity for both the synchronous and the MC cases. The dots are results of numerical simulations, and the solid lines are mean-field diffusivities. The pair of plots at the top (bottom) refer to the fcc-a (fcc-b) configuration of the adsorption energies.

intermediate-high densities. Above this threshold the mutual exclusion causes particles to hinder each other during the motion, thus lowering the diffusivity.

In the second case, indicated as fcc-b, the bridge sites are the deepest ($\varepsilon_B = -10$ kJ mol^{-1} and $\varepsilon_A = 0$). Figure 10 (top right) shows that this causes particles to remain adsorbed in the bridge sites until they reach sufficient energy to jump into the hollow sites. In this case, at the very lowest densities the bridge sites adsorb most of the particles in the system, causing also a hindering effect during migration due to mutual exclusion, which becomes more and more important when the system is

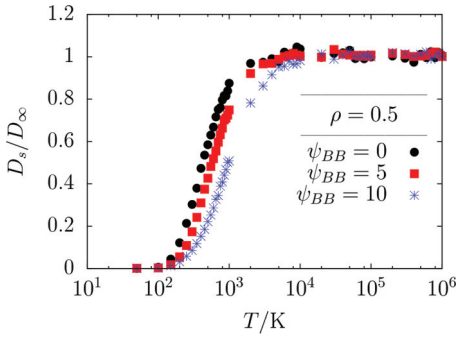

FIG. 11. (Color online) Dependence of self-diffusivity on temperature for three (100) fcc lattices with respectively $\psi_{BB} = 0$, 5, and 10 kJ mol^{-1}. In all cases the overall density is $\rho = 0.5$, $\varepsilon_A = \varepsilon_B = -5$ kJ mol^{-1}, and $\psi_{AB} = \psi_{BA} = 0$. $D_\infty = 5.094 \times 10^{-2}\lambda^2/\tau$ is the self-diffusivity for $T \to \infty$.

loaded with more particles. Therefore, the diffusivity decreases with the overall density.

In Fig. 10 (top), the solid lines refer to a mean-field self-diffusivity estimation (see the Appendix) made by neglecting the correlation effects, that is, assuming that the sequence of particle jumps is a memoryless stochastic process where after each jump the neighborhood of the moving particle randomizes completely according to the global densities ρ_A and ρ_B. This is not true in the numerical simulation, where a particle that just left a site, say r, to enter r' has a higher probability to jump back into r since it is surely empty.

Only for the lowest values of the density is the approximation acceptable (it is exact in the limit of $\rho \to 0$) and it becomes worse with increasing loading. Nevertheless, the comparison between the numerical self-diffusivity D_s and the corresponding mean-field value $\widetilde{D}_s$ is useful to get a measure of the importance of correlations in the migration process, as well as for a comparison between the cases in which prescriptions (ii) and (iii) are present (in the synchronous rule) or absent (in the sequential MC evolution). To this purpose, in the bottom of Fig. 10 we reported the quantities $\widetilde{D}_s/D_s - 1$ and $\widetilde{D}_s^{\mathrm{MC}}/D_s^{\mathrm{MC}} - 1$, i.e., the relative discrepancy between the mean-field and the numerical values of the self-diffusivity at several overall densities, for both the synchronous and the MC cases. As expected, prescriptions (ii) and (iii) cause correlations to be higher in the synchronous case. Moreover, we can see that in the fcc-$b$case the effect of correlations is less pronounced. This is due to the fact that the bridge sites, which in both cases lead to the highest number of directions and thus can be considered as the most responsible for particle diffusion along the lattice, are deeper in the fcc-b case. Analogously to what happened when we lowered the adsorption energy of the homogeneous square lattice from 0 to -10 kJ mol^{-1} (see Fig. 8), the probability of a jump out of every bridge site is less likely to be affected by the the trial directions of the neighboring particles due to prescriptions (ii) and (iii).

As can be seen from the development in Sec. III, the individual migration barriers ψ_{AA}, ψ_{BB}, and ψ_{AB} can be assigned different values, causing the site-to-site mobility to change without modifying the equilibrium distribution of configurations. In Fig. 11 we study the fcc lattice when the barrier for the B-to-B migrations is assigned a nonzero value,

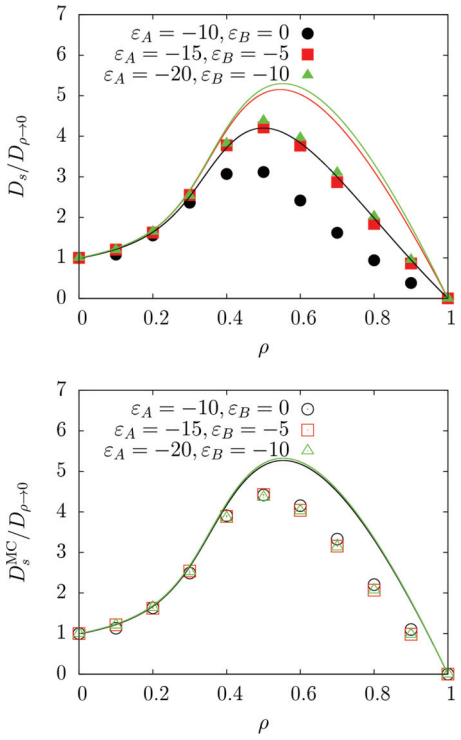

FIG. 12. (Color online) Normalized self-diffusion isotherms for the system fcc-a reported in Fig. 10 compared with the corresponding mean-field isotherms when the adsorption energies are shifted to lower values. The dots are data from numerical simulations (top, synchronous model data; bottom, Monte Carlo data), whereas the solid lines are mean-field data.

while keeping at zero all the other barriers. As expected, the closer ψ_{BB} is to zero, the more the system will be diffusive, whereas the diffusivities will coincide only if temperature is very high—obviously the range of temperatures shown in Fig. 11 is of purely theoretical interest.

In Fig. 12 we compare the sensitivity of the particle mobility to a rescaling of the site adsorption energies reported in the case of synchronous and of sequential evolution. It can be seen that in the synchronous case the shape of the diffusivity vs density curve is more sensitive, thus indicating that prescriptions (ii) and (iii) produce a wider spectrum of possible diffusion profiles for a given system. This can be of remarkable help in coarse-graining problems, when we need to establish a good matching between the lattice-gas diffusion properties and a reference diffusion profile (e.g., experimental or extracted from an atomistic simulation). Moreover, Fig. 12 shows that also the shape of the mean-field diffusion isotherm changes with the site adsorption energies. This implies that the relative amount of autocorrelations does not change significantly when the sites are made more strongly binding. In other words, the synchronous algorithm preserves its natural correlations. This is an important point in the modeling of diffusion on a surface with strong adsorption energies, when we do not want the correlations appearing in the single-particle motion on the reference system to get lost when we represent it with a coarse-grained model.

Finally, for strongly adsorbing sites the simulation of diffusion with the synchronous rule turns out to be less time consuming than the sequential case. Let us see how. From Eq. (34) we see that the more negative ε is, the closer the acceptance of a move in the synchronous rule will get to the acceptance of the corresponding Arrhenius jump in the MC algorithm. Equation (34) refers to a homogeneous system, but if all the sites are strongly adsorbing, that consideration is valid for a heterogeneous lattice as well. We can observe this fact in Fig. 12, where the synchronous and the MC versions of the fcc surface with $\varepsilon_A = -20$ and $\varepsilon_B = -10$ kJ mol^{-1} produce very similar diffusivities. Since in this case the average number of accepted moves is comparable between synchronous and MC rule, we can also compare the two algorithms in terms of efficiency. For the MC case, at each time step the random number generator must be called $N - 1$ times (with N the number of particles) to establish the sequence by which the particles will be invoked for a jump attempt, plus N times needed to select the random directions, for a total of $2N + 1$ calls of the random number generator. For the synchronous case the particles do not need to be invoked randomly; therefore for each time step only N random generator calls are required. This means that a run of the synchronous system requires approximately one-half of the random generator calls needed by the corresponding MC run.

V. CONCLUSIONS

We have shown that a synchronous rule for particle jumps on a lattice, although obtained through the manipulation of a glass-forming sequential rule and containing prescriptions that are necessary solely to ensure that detailed balance, mutual exclusion, and fully synchronous update of the lattice sites coexist without conflicts, produces normal diffusion. We compared the results with the ones obtained by a sequential Monte Carlo algorithm and observed that the diffusion produced in the synchronous rule is generally lower than the MC counterpart (they are strictly equal only in the limit of infinite dilution) and with stronger correlations. The shape of the diffusion isotherms obtained through simulation of the synchronous rule is shown to be more sensitive to changes in the parameters than the MC case, and the two methods produce nearly equivalent results if the lattice sites are strongly adsorbing. Moreover, in the latter case the simulation of the synchronous rule is less computationally expensive than the corresponding MC run. This approach can therefore be conveniently used for the simulation of strongly correlated migration processes like the ones observed in confined systems. Further possible developments of the synchronous rule are the implementation of lateral interactions in the lattice Hamiltonian without violating the detailed balance, the diffusion of multiple species, the application of the rule to nanoconfined systems, and the proper modification of the rule to recover a glassy behavior.

ACKNOWLEDGMENTS

F.G.P. is thankful to Regione Autonoma della Sardegna for the financial support provided within the Progetto Unico di Ateneo “Assegni di Ricerca” — POR FSE 2007/2013 (Asse IV - Capitale Umano - Obiettivo Operativo I.3 - Linea di attività I.3.1).

APPENDIX: MEAN-FIELD UNCORRELATED SELF-DIFFUSIVITY

Neglecting memory effects in the migration process of a tagged particle, the self-diffusion coefficient in a two-dimensional lattice-gas can be approximated as [36]

$$\widetilde{D}_s = \frac{1}{4\tau}\langle \delta r^0 \cdot \delta r^0 \rangle, \tag{A1}$$

where δr^0 is the displacement performed by the particle as a consequence of the jump performed at time $t = 0$, which is strictly connected to the probability of escaping an adsorption site. In the case of a (100) fcc surface, the escape probability varies depending on which kind of site the particle is adsorbed from time to time. As can be seen in Fig. 9, there are two kinds of sites with different adsorption energies and connectivities. From a site of type A (that the particle occupies with probability $\rho_A/3\rho$), the particle will jump into one out of the four neighboring sites (of type B) with probability $J_A^{\rightarrow}$. Such a jump will cause the square of the displacement to be $\delta r^0 \cdot \delta r^0 = \lambda^2$. From a site of type B (that the particle occupies with probability $2\rho_B/3\rho$), the particle will jump into one out of the two neighboring sites of type A with probability $J_B^{\rightarrow}$, causing the squared displacement to be $\delta r^0 \cdot \delta r^0 = \lambda^2$, or into one out of the four neighboring sites of type B with probability $J_B^{\nearrow}$, causing the squared displacement to be $\delta r^0 \cdot \delta r^0 = 2\lambda^2$. Taking into account all three rule prescriptions, these probabilities read

$$J_A^{\rightarrow} = \frac{e^{\beta(\varepsilon_A-\psi_{AB})}}{\nu_{\max}}(1-\rho_B)\left(1-\rho_A\frac{e^{\beta(\varepsilon_A-\psi_{AB})}}{\nu_{\max}}\right) \times\left(1-\rho_B\frac{e^{\beta(\varepsilon_B-\psi_{BB})}}{\nu_{\max}}\right)^2\left(1-\rho_B\frac{e^{\beta(\varepsilon_B-\psi_{BA})}}{\nu_{\max}}\right) \times\left(1-\rho_B\frac{e^{\beta(\varepsilon_B-\psi_{BA})}+e^{\beta(\varepsilon_B-\psi_{BB})}}{\nu_{\max}}\right)^2, \tag{A2}$$

where the last term takes account of the fact that there are two B sites, in the neighborhood of an A site, which can point to either the departure or the destination site of the jumping particle,

$$J_B^{\rightarrow} = \frac{e^{\beta(\varepsilon_B-\psi_{BA})}}{\nu_{\max}}(1-\rho_A)\left(1-\rho_B\frac{e^{\beta(\varepsilon_B-\psi_{BA})}}{\nu_{\max}}\right) \times\left(1-\rho_A\frac{e^{\beta(\varepsilon_A-\psi_{AB})}}{\nu_{\max}}\right)\left(1-\rho_B\frac{e^{\beta(\varepsilon_B-\psi_{BB})}}{\nu_{\max}}\right)^2 \times\left(1-\rho_B\frac{e^{\beta(\varepsilon_B-\psi_{BA})}+e^{\beta(\varepsilon_B-\psi_{BB})}}{\nu_{\max}}\right)^2, \tag{A3}$$

where, again, the last term is due to the possibility of two B neighbors of the B-type departure site pointing to either the departure or the destination site, and

$$J_B^{\nearrow} = \frac{e^{\beta(\varepsilon_B-\psi_{BB})}}{\nu_{\max}}(1-\rho_B)\left(1-\rho_B\frac{e^{\beta(\varepsilon_B-\psi_{BB})}}{\nu_{\max}}\right)^4 \times\left(1-\rho_A\frac{e^{\beta(\varepsilon_A-\psi_{AB})}}{\nu_{\max}}\right)^2\left(1-2\rho_A\frac{e^{\beta(\varepsilon_A-\psi_{AB})}}{\nu_{\max}}\right). \tag{A4}$$

Here, instead, the last term takes account of the fact that one A neighbor of the B-type departure site can point to either the departure or the destination site. The mean-field expression for $\langle \delta r^0 \cdot \delta r^0 \rangle$ reads then

$$\langle \delta r^0 \cdot \delta r^0 \rangle = \frac{4\lambda^2}{3\rho}[\rho_A J_A^{\rightarrow} + \rho_B(4J_B^{\nearrow} + J_B^{\rightarrow})], \tag{A5}$$

which, inserted in Eq. (A1), provides the mean-field diffusivity plotted in Fig. 10 (top, solid line).

[1] B. Chopard and M. Droz, *Cellular Automata Modeling of Physical Systems*, 1st ed. (Cambridge University Press, Cambridge, England, 1998).

[2] J. Hardy, Y. Pomeau, and O. de Pazzis, Phys. Rev. A **13**, 1949 (1976).

[3] U. Frisch, B. Hasslacher, and Y. Pomeau, Phys. Rev. Lett. **56**, 1505 (1986).

[4] D. d. P. Lallemand and U. Frisch, Europhys. Lett. **2**, 291 (1986).

[5] U. Frisch, D. d'Humières, B. Hasslacher, P. Lallemand, Y. Pomeau, and J.-P. Rivet, Complex Syst. **1**, 649 (1987).

[6] J.-P. Rivet and J. P. Boon, *Lattice Gas Hydrodynamics*, 1st ed. (Cambridge University Press, Cambridge, England, 2001).

[7] D. Dab, A. T. Lawniczak, J. P. Boon, and R. Kapral, Phys. Rev. Lett. **64**, 2462 (1990).

[8] J. P. Boon, D. Dab, R. Kapral, and A. T. Lawniczak, Phys. Rep. **273**, 55 (1996).

[9] T. Toffoli and N. Margolus, Physica D **45**, 229 (1990).

[10] T. Toffoli and N. Margolus, *Cellular Automata Machines: A New Environment for Modeling*, 1st ed. (MIT Press, Cambridge, MA, 1997).

[11] R. C. Tolman, *The Principles of Statistical Mechanics* (Oxford University Press, Oxford, 1938).

[12] N. Metropolis, A. W. Rosenbluth, M. N. Rosenbluth, A. H. Teller, and E. Teller, J. Chem. Phys. **21**, 1087 (1953).

[13] W. K. Hastings, Biometrika **57**, 97 (1970).

[14] A. J. Bray, Adv. Phys. **43**, 357 (1994).

[15] M. P. Allen and D. J. Tildesley, *Computer Simulation of Liquids* (Oxford University Press, Oxford, 1989).

[16] D. Frenkel and B. Smit, *Understanding Molecular Simulations—From Algorithms to Applications*, 2nd ed. (Academic Press, London, 2002).

[17] K. Froböse and J. Jäckle, J. Stat. Phys. **42**, 551 (1986).

[18] F. G. Pazzona, P. Demontis, and G. B. Suffritti, J. Chem. Phys. **131**, 234704 (2009).

[19] M. Hildebrand and A. S. Mikhailov, J. Phys. Chem. **100**, 19089 (1996).

[20] D. G. Vlachos and M. A. Katsoulakis, Phys. Rev. Lett. **85**, 3898 (2000).

[21] R. Lam, T. Basak, D. G. Vlachos, and M. A. Katsoulakis, J. Chem. Phys. **115**, 11278 (2001).

[22] B. Chopard, A. Masselot, and M. Droz, Phys. Rev. Lett. **81**, 1845 (1998).
[23] K. Hahn and J. Kärger, J. Phys. Chem. **100**, 316 (1996).
[24] R. Yamamoto and A. Onuki, Phys. Rev. E **58**, 3515 (1998).
[25] D. Richter, B. Frick, and B. Farago, Phys. Rev. Lett. **61**, 2465 (1988).
[26] A. C. Pan, J. P. Garrahan, and D. Chandler, Phys. Rev. E **72**, 041106 (2005).
[27] I. Vattulainen, S. C. Ying, T. Ala-Nissila, and J. Merikoski, Phys. Rev. B **59**, 7697 (1999).
[28] T. Ala-Nissila, R. Ferrando, and S. C. Ying, Adv. Phys. **51**, 949 (2002).
[29] D. Dubbeldam, E. Beerdsen, T. J. H. Vlugt, and B. Smit, J. Chem. Phys. **122**, 224712 (2005).
[30] D. A. Reed and G. Ehrlich, Surf. Sci. **102**, 588 (1981).
[31] P. Demontis, F. G. Pazzona, and G. B. Suffritti, J. Chem. Phys. **126**, 194710 (2007).
[32] A. A. Tarasenko and L. Jastrabík, Surf. Sci. **507–510**, 108 (2002).
[33] T. Zambelli, J. Trost, J. Wintterlin, and G. Ertl, Phys. Rev. Lett. **76**, 795 (1996).
[34] Z. Chvoj, H. Conrad, V. Cháb, M. Ondrejcek, and A. M. Bradshaw, Surf. Sci. **329**, 121 (1995).
[35] Z. Chvoj, H. Conrad, and V. Cháb, Surf. Sci. **376**, 205 (1997).
[36] F. G. Pazzona, A. Gabrieli, A. M. Pintus, P. Demontis, and G. B. Suffritti, J. Chem. Phys. **134**, 184109 (2011).